A quantitative evaluation of the structure and properties of the methyl ester of divinyl ether - maleic anhydride 1:2 copolymer*

Robert J. Samuels
Hercules Incorporated, Research Center, Wilmington, Delaware 19899, USA
(Received 8 September 1976; revised 3 November 1976)

The methyl ester of divinyl ether–maleic anhydride 1:2 copolymer (DME) has been used as a molecular probe to identify the structure of DIVEMA (divinyl ether–maleic anhydride 1:2 copolymer). Solution light scattering, gel permeation chromatography, and intrinsic viscosity measurements have shown that tetrahydrofuran at 30°C is a theta solvent for DME, and that DME has a random coil conformation with possible long chain branching at higher molecular weights. Determination of the characteristic ratio of DME required identification of its molecular structure. Molecular model studies revealed that the bulky methyl ester groups cause much more steric hindrance in the generally accepted tetrahydropyran structure of DME than in an alternative tetrahydrofuran structure. This observation, together with the polymer solution measurements, indicates the latter structure is more in accord with experimental data, suggesting that both DME and the parent DIVEMA contain tetrahydrofuran in their structures.

INTRODUCTION

The polyanion, 1:2 divinyl ether–maleic anhydride cyclic alternating copolymer (DIVEMA), is a biologically active synthetic polymer. It has anti-tumour activity; it induces the formation of interferon; it has antiviral, antibacterial, and antifungal activity; it is an anticoagulant and an anti-inflammatory agent. DIVEMA is an immunopotentiator: it increases the rate of phagocytosis, it activates macrophages selectively, and it inhibits RNA-dependent DNA polymerase[1,2]. The broad spectrum of biological activity of this polymer invites investigation into the structural characteristics that influence its behaviour. Of particular interest are its molecular structure, molecular weight, and molecular weight distribution.

A direct characterization of the molecular weight and molecular weight distribution of DIVEMA presented problems. Attempts made to carry out gel permeation chromatography (g.p.c.) on solutions of the anhydride in organic solvents using Styragel columns were unsuccessful, presumably because of partial hydrolysis of the anhydride groups[3]. Attempts to fractionate solutions of the free acid in aqueous salt solution by g.p.c. were also unsuccessful[3]. Similar problems were encountered by Butler and Wu[4].

In order to circumvent these problems the DIVEMA samples were converted into their methyl esters. This was accomplished by first refluxing the DIVEMA samples in methanol and then treating them with diazomethane; several diazomethane treatments were necessary to obtain complete esterification[1,2]. These esters fractionated smoothly on a Styragel column using tetrahydrofuran as solvent. A comparison of the molecular weights of the anhydride and the methyl ester both by membrane osmometry and by light scattering demonstrated that no appreciable degradation had occurred during the esterification[1,2].

With the availability of the stable methyl ester of divinyl ether–maleic anhydride 1:2 copolymer (DME) it was now possible to evaluate the dilute solution characteristics of the DME polymer, and to develop a g.p.c. technique for determining its molecular weight and molecular weight distribution. This required the use of both narrow fractions of DME, and the application of Benoit's universal calibration technique[5].

With reliable solution data on DME fractions, an evaluation of the molecular structure of DME was also possible. Methyl esterification of DIVEMA acts as a molecular probe for differentiating different molecular precursor models of DIVEMA. It has been found that DME and hence its precursor DIVEMA, must both be considered to contain tetrahydrofuran rings and not, as is generally accepted[6,7], primarily tetrahydropyran rings. The following is a report of these studies.

EXPERIMENTAL

The DME samples used in this study are reported elsewhere[1,2]. The narrow molecular weight distribution, standard polystyrene samples were obtained from several sources, including Dow, Waters Associates, and Utopia. DME fractions were obtained from Waters Associates, who fractionated a large DME sample in their preparative g.p.c. using Styragel columns with methylene chloride as solvent.

Viscosity measurements of both polystyrene and DME were made in an automatic capillary flow viscometer in THF solutions at 30°C.

* Presented at the First Cleveland Symposium on Macromolecules, Structure and Properties of Biopolymers, Case Western Reserve University, Cleveland, Ohio, USA, October 1976.

Light scattering measurements for the determination of $\bar{M}_w$ were carried out in acetone at 25°C for DME and in THF at 25°C for polystyrene using a Sofica light scattering photometer. The scattered intensities, measured as a function of concentration and scattering angle θ were analysed by Zimm's equation:

$$\frac{Kc}{R} = \frac{1}{\bar{M}_w}\left[1 + \frac{1}{3}\left(4\frac{\pi M_0}{\lambda_0}\right)^2 R_g^2 \sin^2(\theta/2)\right] + 2A_2C \quad (1)$$

where C is the polymer concentration, g/ml; A_2 is the second virial coefficient, mol cm^3/g^2; R_g is the polymer radius of gyration, Å; R is Rayleigh's ratio, calculated from the excess scattering of the polymer in solution and K is a constant, determined by the optical parameters of the polymer and solvent.

A Waters Associates GPC Model 100 was used for the gel permeation chromatography (g.p.c.) measurements. It was operated at 30°C using tetrahydrofuran (THF) as solvent. The Styragel column sequence was, $>5 \times 10^6$, 1.5×10^5–7×10^5, 5×10^3–1.5×10^4, and 5×10^3–1.5×10^4. A flow rate of 1 ml/min was maintained. Injections were for two minutes.

Several features of the computer characterization of the g.p.c. data should be mentioned. Conventionally, the volume at which the peak of each g.p.c. curve occurs is plotted against the weight-average molecular weight to obtain a calibration curve. Two problems arise from this convention however: (a) the peak position represents the $\bar{M}_w$ value only for a symmetrical curve, and (b) only one point (the peak) of the complete g.p.c. curve is utilized for the calibration. Marks[8] has developed a system for circumventing these problems. An arbitrary molecular weight vs. elution volume (counts) calibration curve is set up. This calibration curve is then adjusted by an iterative technique to best fit all of the known polystyrene data. In this way, the complete g.p.c. curve of each fraction is used in the evaluation; an approach which also yields the integral volume count at which the known $\bar{M}_w$ emerges from the g.p.c. This integral volume count position is chosen for the calibration. It represents the peak position of the g.p.c. curve only when the symmetry of the g.p.c. curve justifies such a choice.

The solid calibration curve used in this study was best fitted to the experimental points using a function consisting of an inverse tangent plus a negative sloped straight line. This function has the S shape characteristic of a cubic equation and is asymptotic to two sloped parallel lines. It was chosen to satisfy the following three criteria: (a) the extrapolation should not be arbitrarily adjusted to improve results, (b) a simple smooth function is preferred, and (c) the calibration procedure should use the same method of calculation as is used for the sample, e.g. use the integral equations rather than the peak maximums. The function sometimes needs constraints on the asymptotic slope, and for this reason has the form:

$$(\bar{M}_w)_v = b_0 + b_1\left\{b_2 v + \frac{1-b_2}{b_3}\tan^{-1}[b_3(v-b_4)]\right\} \quad (2)$$

which has the derivative:

$$\frac{d(M_w)_v}{dv} = b_1\left\{b_2 + \frac{1-b_2}{1+b_3^2(v-b_4)^2}\right\} \quad (3)$$

At $v = \pm\infty$, the slope is b_1b_2 and at $v = b_4$, the slope is b_1. We are currently constraining $b_2 \leqslant 2.5$ so that the asymptotic slope must be equal to or less than two and a half times the slope at the critical point. This same functional form is used for the $([\eta]\bar{M}_w)$ calibration curve.

RESULTS AND DISCUSSION

The purpose of this study is (A) to determine the solution properties of the methyl ester of divinyl ether–maleic anhydride 1:2 copolymer, (DME); (B) to develop a g.p.c. system for characterizing DME; and (C) to use this information to evaluate the molecular structure of DME. In order to accomplish (B), it was necessary to obtain and evaluate fractions of DME, and to augment these data with standard polystyrene results through the mechanism of the universal calibration technique developed by Benoit[5].

(A) Solution properties of DME

Characterization of DME fractions. A large sample of DME was prepared and sent to Waters Associates, Inc., for fractionation in their preparative g.p.c. The sample was fractionated on Styragel columns using methylene chloride as solvent. Nine of the fractions were large enough to use for evaluation of intrinsic viscosities, weight-average molecular weights, and g.p.c. analysis. Evaluation of batch DME in our analytical g.p.c. showed that tetrahydrofuran (THF) was a better solvent to use with the Styragel columns and all subsequent work used THF as solvent. It is interesting to note that Butler and Wu[4] suggested THF could be used as the g.p.c. carrier for DME even though they did not use this system themselves.

The intrinsic viscosity of the nine DME fractions was determined in THF at 30°C (*Figure 1* and *Table 1*). The weight-average molecular weight of these same fractions was determined in acetone to take advantage of the better (dn/dc) of this solvent (*Table 1*). The intrinsic viscosity–weight-average molecular weight relationship for DME in THF at 30°C was then determined (*Figure 2*) as:

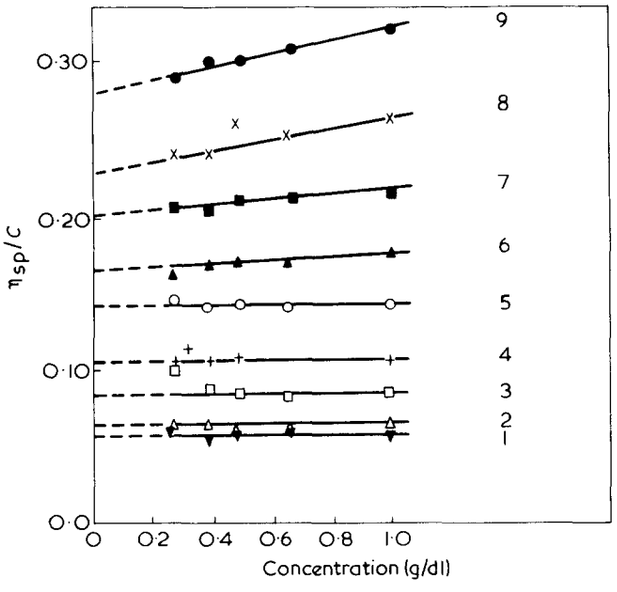

Figure 1 Intrinsic viscosity of DIVEMA methyl ester (DME) fractions 1–9 in THF at 30°C

Table 1 Solution data for the DME fractions

Designation	$[\eta]_{THF}^{30°C}$ (dl/g)	$\bar{M}_w^a$ x 10^{-3}	$\bar{M}_v^b$ x 10^{-3}	$(A_2\bar{M}_w^2)$ x 10^{-6} (cm³/mol)
9	0.282	543.0	353.2	24.9
8	0.231	275.0	251.8	12.9
7	0.202	183.0	145.7	8.86
6	0.164	117.0	107.2	3.58
5	0.142	75.5	68.9	2.25
4	0.106	43.8	43.6	0.70
3	0.085	28.6	27.2	0.34
2	0.065	20.4	16.3	0.16
1	0.058	15.4	10.6	0.13

a Determined by light scattering in acetone at 25°C.
b Calculated from g.p.c. in THF at 30°C

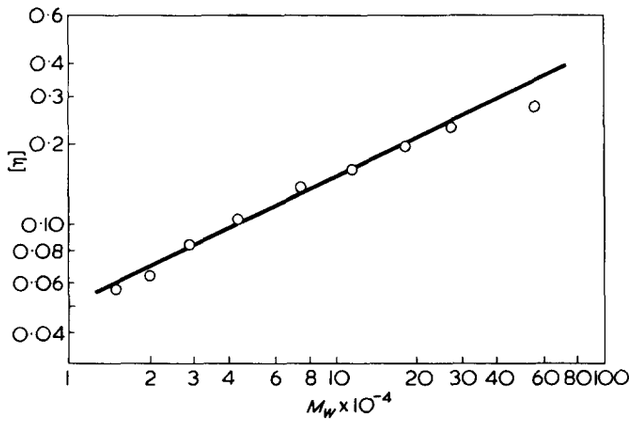

Figure 2 Intrinsic viscosity–molecular weight relationship for DME fractions in THF at 30°C, $[\eta]_{THF}^{30°C} = 4.895 \times 10^{-4} \bar{M}_w^{0.5}$

$$[\eta]_{DME} = 4.895 \times 10^{-4} \bar{M}_w^{0.50} \quad (4)$$

Thus THF at 30°C seems to be acting as a theta solvent for DME.

The structure of DME is not completely known and one question that arises is whether the polymer molecule is branched or linear. Since maleic anhydride copolymerizes well with vinyl ethers, a dangling vinyl ether group could act as a branch point, leading to long chain branching.

For a linear molecule the Mark–Houwink equation takes the form:

$$[\eta]_l = KM^a \quad (5)$$

Long chain branched molecules in solutions are more compact than the equivalent linear molecule of the same molecular weight. For this reason, the intrinsic viscosity of a branched molecule of a given molecular weight will be less than that of an equivalent molecular weight linear molecule under the same experimental conditions. A branching factor, g, which represents this hydrodynamic volume change due to chain branching can be defined as[9]:

$$g^{1/2} = [\eta]_{branched}/[\eta]_{linear} \quad (6)$$

Combining equations, the Mark–Houwink equation for branched molecules becomes:

$$[\eta]_{branched} = KM^a g^{1/2} \quad (7)$$

For a linear molecule in a theta solvent, $a = 0.5$. This exponent was obtained for DME in THF at 30°C and suggests that DME is indeed linear. However, the higher molecular weight region of the plot in *Figure 2* shows some curvature to lower values. *Figure 3* shows the deviation of the experimental points in *Figure 2* from the solid line, in the form of the branching factor $g^{1/2}$, plotted against the weight-average molecular weight of each sample. The two highest molecular weight samples show $g^{1/2}$ values outside the average scatter of the points, suggesting some long chain branching may occur at these higher molecular weights. Considering that higher molecular weight fractions of DIVEMA have shown different biological behaviour than the lower molecular weight material, this observation could be significant.

Further support for this interpretation is given by the light scattering data. *Figure 4* shows a log–log plot of $(A_2\bar{M}_w^2)$ vs. $\bar{M}_w$, where A_2 is the second virial coefficient of the fraction as determined by light scattering in acetone. $(A_2\bar{M}_w^2)$ is proportional to the excluded volume of the sample[10] and would be expected to be smaller for a branched molecule than for a linear molecule of the same molecular

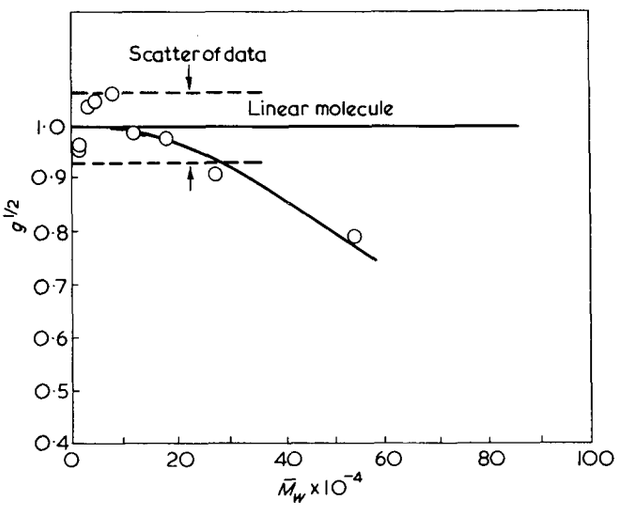

Figure 3 Effect of molecular weight on the degree of branching in DME

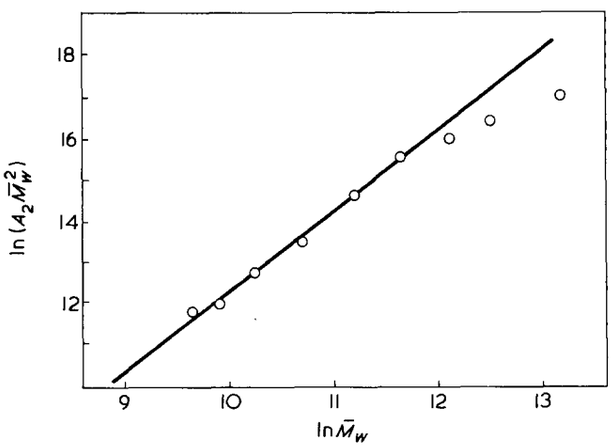

Figure 4 The change in the excluded volume term $(A_2\bar{M}_w^2)$ with molecular weight for the DME fractions measured in acetone

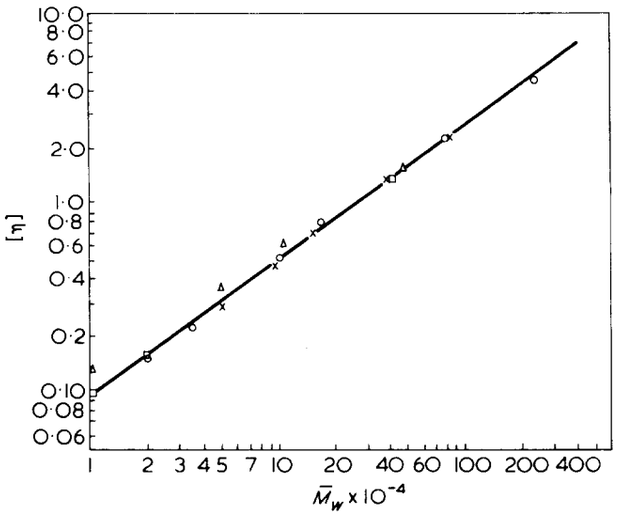

Figure 5 Determination of the intrinsic viscosity–weight-average molecular weight relation for polystyrene standards in THF at 30°C. $[\eta] = 1.328 \times 10^{-4} \bar{M}_w^{0.713}$. ○, Experimental $\bar{M}_w$ and $[\eta]$; □, experimental $[\eta]$, reported $\bar{M}_w$; X, data of Boni *et al.*[11]; △, data of Coleman and Fuller[12]

weight. As can be seen in *Figure 4*, the same deviation from linearity is observed for the $(A_2\bar{M}_w^2)$ values of the two highest molecular weight samples in acetone as was observed for $[\eta]$ in THF. Namely, the $(A_2\bar{M}_w^2)$ values of these samples are lower than would be expected for that molecular weight, again suggesting some long chain branching may be present.

Characterization of polystyrene fractions. The molecular weight range of the DME fractions is not wide enough to adequately characterize a g.p.c. calibration curve for bulk polymer. If the DME has a random coil conformation, and the Mark–Houwink constants are known for the same solvent conditions as are present in the g.p.c. column, then a universal calibration curve could be used. Calibration over a wider molecular weight range could then be made using narrow molecular weight distribution polystyrene standards, and a reliable DME calibration curve extracted using the appropriate Mark–Houwink constants.

The intrinsic viscosity of nine narrow molecular weight distribution polystyrene standards were measured in THF at 30°C. The weight-average molecular weight of six of these standards was measured in THF (*Figure 5*), while the weight-average molecular weight reported by the supplier was used for the additional three samples. The resulting data, plotted in *Figure 5*, yielded the Mark–Houwink relation:

$$[\eta]_{PS} = 1.328 \times 10^{-4} \bar{M}_w^{0.713} \quad (8)$$

This result agrees very well with data of Boni *et al.*[11] obtained in THF at 23°C (*Figure 5*). Some recent limited data of Coleman and Fuller[12] deviates from these results (*Figure 5*). No explanation for their deviation exists at present. It is interesting to note however that their molecular weights were determined in methyl ethyl ketone (no temperature reported) while the present data was obtained in THF at 25°C.

(B) The g.p.c. universal curve for DME

The universal calibration curve concept calls attention to the fact that, since molecules separate by volume in the g.p.c., samples of different polymers having the same coil size will elute at the identical elution volume. If this is true, then a plot of coil size against elution volume (V_p) should be the same for all polymers measured under the same solvent, temperature, and column conditions. Also, once it is shown that a polymer fits the universal calibration curve, any other more accessible polymer that also fits that curve can be used as a calibrating standard for the columns.

Benoit[5] was the first one to recognize this simple concept. He demonstrated that if one did not plot $\log \bar{M}_w$ vs. V_p as a calibration for g.p.c., but instead $\log([\eta]\bar{M}_w)$ against V_p, a universal curve would be obtained. The reason for this is that theoretically (for random coils):

$$([\eta]\bar{M}_w) = \phi R^3 \quad (9)$$

where ϕ is Flory's universal constant, and R^3 is the cube of the radius of the coil (and hence a volume term).

Since, the intrinsic viscosity is described by the Mark–Houwink equation:

$$[\eta] = K\bar{M}^a \quad (10)$$

where K and a are constants depending on the polymer, solvent, and temperature, then:

$$[\eta]\bar{M}_w = K\bar{M}_w^{1+a} = \phi R^3 \quad (11)$$

This means the molecular volume of a given molecular weight sample in solution will depend on the solvent–polymer interaction of that polymer. Thus, experimentally, different polymers of the same molecular weight but different solvent–polymer interaction parameters will have different volumes under the same conditions of solvent and temperature. These polymers will have different calibration curves when plotted in terms of $\bar{M}_w$ since the same molecular weight will have a different volume and hence appear at a different V_p. When these same polymers are plotted as $\log([\eta]\bar{M}_w)$ vs. V_p they will fall on the same calibration curve, since identical $([\eta]\bar{M}_w)$ values for each polymer represent identical volumes and hence they will elute at the same V_p.

An interesting feature of the universal calibration curve has been reported by Ambler and McIntyre[13]. They found that $([\eta]\bar{M}_w)$ will serve as a universal calibration parameter only when the molecular geometries of all of the samples involved are similar, e.g. they are all flexible Gaussian coils, or they are all rigid rods. Since polystyrene is being used as the calibration standard, correspondence of the DME fractions with the polystyrene data would indicate DME has a Gaussian coil conformation in solution.

Figure 6 is a universal plot of the polystyrene and DME fraction data in THF at 30°C. The solid line is the best line drawn by the computer through the polystyrene data only. The DME points were not used in calculating the universal curve. As can be seen, the DME fractions fit the universal curve quite well, indicating DME has a Gaussian coil conformation in THF solution at 30°C.

With the parameters for the universal curve determined using polystyrene as a standard, the DME fractions shown to fit the same universal curve (*Figure 6*), and the K and a values for polystyrene and DME known, the $\bar{M}_w$ calibration curve for DME can be calculated. The calculated calibration curve for DME is shown in *Figure 7*. The experimental DME data are also plotted. A good fit is obtained. This DME calibration curve is now based on experimental data over a

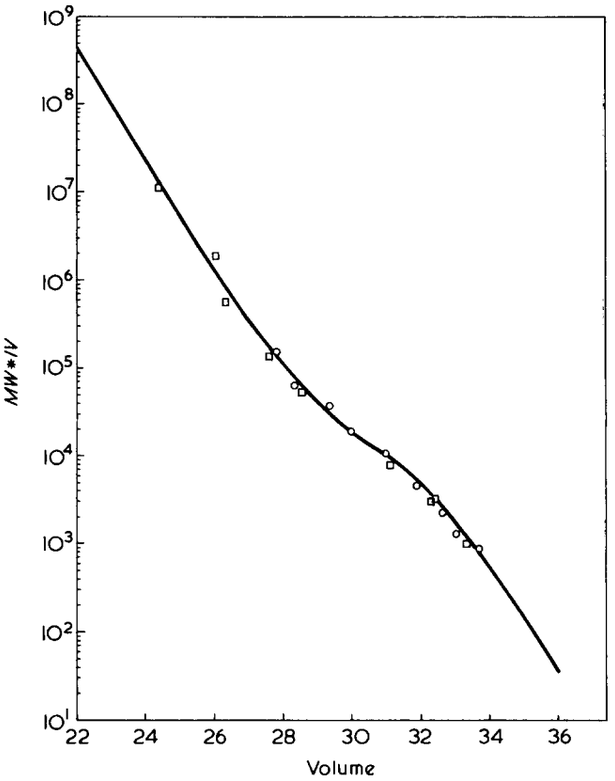

Figure 6 Universal calibration curve obtained from the polystyrene data only. The experimental polystyrene and DME data are included on the curve: □, PS; ○, DME

$\bar{M}_w$ range of 2.5×10^6 to 1.0×10^4, rather than the much more limited range of 5.4×10^5 to 1.5×10^4, through the use of polystyrene standards and the universal curve concept. The g.p.c. curves for the Waters fractions are shown in *Figure 8*.

(C) Evaluation of the molecular structure of DME

The characteristic ratio, C_∞, gives a measure of chain flexibility. It is used as a basis for comparing the average dimensions of various random coil chains[14]. In the limit for long chains:

$$C_\infty = \left(\frac{\langle r^2\rangle_0}{M}\right)_\infty \left(\frac{M_b}{l^2}\right) \tag{12}$$

where $\langle r^2\rangle_0$ is the root-mean-square end-to-end distance of the polymer chain in the unperturbed state, M is the molecular weight of the chain, M_b is the mean molecular weight per flexible skeletal bond, and l is the length between flexible bonds. For chains containing rigid elements in their backbone, rotation occurs around 'virtual bonds', i.e. rotation occurs not around each bond in the backbone but instead around equivalent chains consisting of a smaller number of rigid 'statistical chain elements' of length l, which are freely joined to each other.

In a theta solvent:

$$[\eta]_\theta = K_\theta \bar{M}_v^{1/2} \tag{13}$$

Here $[\eta]_\theta$ is the intrinsic viscosity, $\bar{M}_v$ is the viscosity-average molecular weight of the polymer, and K_θ is a constant. Flory has shown[14] that under θ conditions:

$$(\langle r^2\rangle_0/M)_\infty = (K_\theta/\phi)^{2/3} \tag{14}$$

where ϕ, at or near the θ point, has a constant value of 2.6×10^{21}.

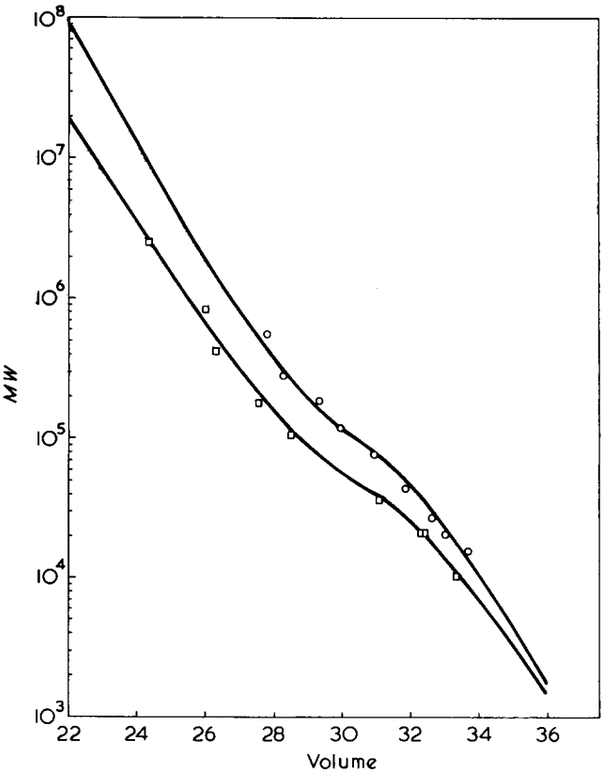

Figure 7 M_W vs. elution volume curves for polystyrene and DME calculated from the universal calibration curve and the experimental K and a values. The experimental polystyrene and DME data are included on the curves: □, PS; ○, DME

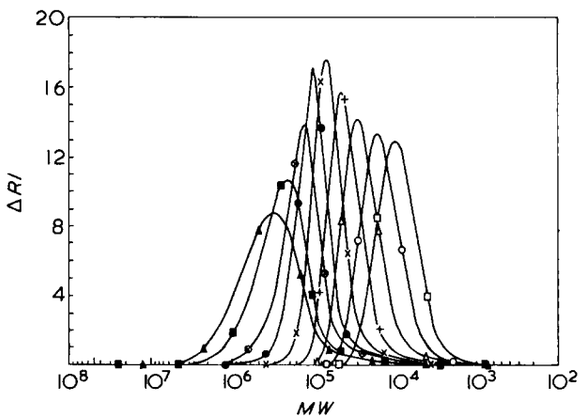

Figure 8 G.p.c. curves for the DME fractions obtained from the Waters preparative g.p.c. separation:

Designation	$\overline{MW}$	$\overline{MN}$	Ratio
▲ 9	423 049	157 068	2.693
■ 8	293 227	115 042	2.549
⊕ 7	159 002	96 597	1.646
● 6	114 941	80 237	1.433
× 5	74 566	57 609	1.294
+ 4	48 013	35 989	1.334
△ 3	29 962	19 862	1.508
○ 2	17 512	12 319	1.422
□ 1	11 152	7 764	1.436

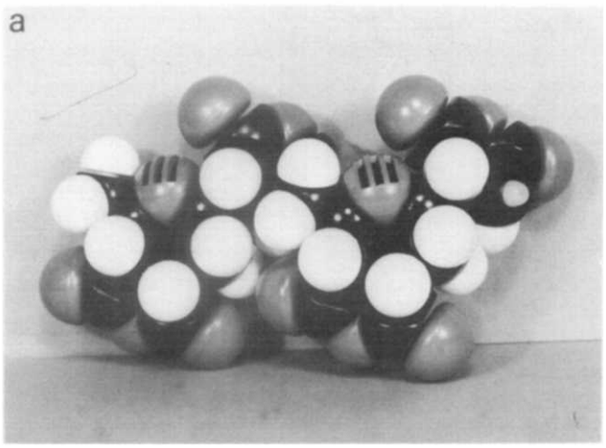

Figure 9 The molecular structure of DIVEMA(I): (a) Ealing CPK atomic model showing 2 monomer units; (b) schematic representation of 2 monomer units

Normally, K_θ values are obtained by converting the measured $\bar{M}_w$ values to $\bar{M}_v$ values by assuming the polymer has a most probable distribution and applying the equation; $\bar{M}_v/\bar{M}_w = [(1+a)\,\Gamma(1+a)]^{1/a}/2$, where a is the exponent of the Mark–Houwink equation obtained from a $[\eta] - \bar{M}_w$ plot. This assumption of a most probable distribution can lead to error and is best avoided. The $\bar{M}_v$ values for the DME fractions were determined explicitly in the g.p.c. and thus polydispersity assumptions are avoided. The DME expression takes the form:

$$[\eta]_\theta = K_\theta \bar{M}_v^{1/2} = 5.239 \times 10^{-4}\, \bar{M}_v^{1/2} \qquad (15)$$

This leads to a value of $(\langle r^2\rangle_0/M)_\infty$ of:

$$(\langle r^2\rangle_0/M)_\infty = (K_\theta/\phi)^{2/3} = 34.36 \times 10^{-18}\ \text{cm}^2\ \text{mol/g} \qquad (16)$$

The characteristic ratio, C_∞, can now be calculated provided a realistic calculation of (M_b/l^2) can be made.

The widely accepted form of DIVEMA is[6,7] (*Figure 9*):

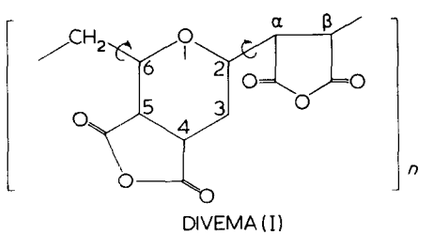

DIVEMA (I)

Upon esterification DIVEMA (I) would then be expected to convert to the methyl ester form (*Figure 10*):

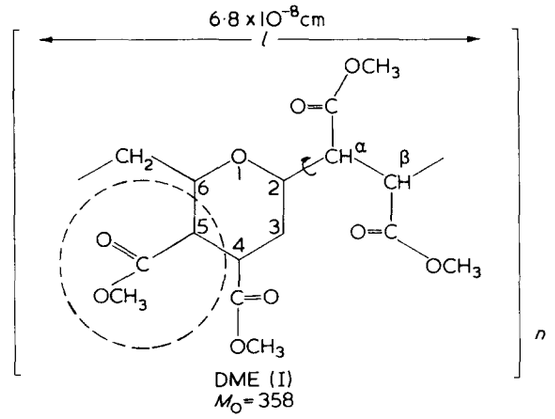

If one considers the whole comonomer DME(I) unit as a rigid 'virtual bond' then $M_b = 358$, $l = 6.8 \times 10^{-8}$ cm and C_∞ equals 2.65. The characteristic ratios, C_∞, for polymers usually are in the range 4 to 10. The theoretical value for free rotation is 2.0. Stiffer, more bulky molecules have high values of C_∞ while a flexible chain such as polyoxyethylene has the lowest reported C_∞ value for real chains of 4. Clearly, a calculated C_∞ value for the bulky DME molecule of 2.65 is unreasonable.

The unreasonable C_∞ value obtained for DME(I), when the whole unit is considered as a single 'virtual' bond, suggests some smaller flexible subunit of the molecule should be considered. A model containing two monomer units of DIVEMA(I) was constructed using Ealing CPK atomic models (*Figure 9*). Bond rotation was found to be difficult but possible around both the 2- and 6-positions of the six-membered tetrahydropyran ring in the DIVEMA(I) struc-

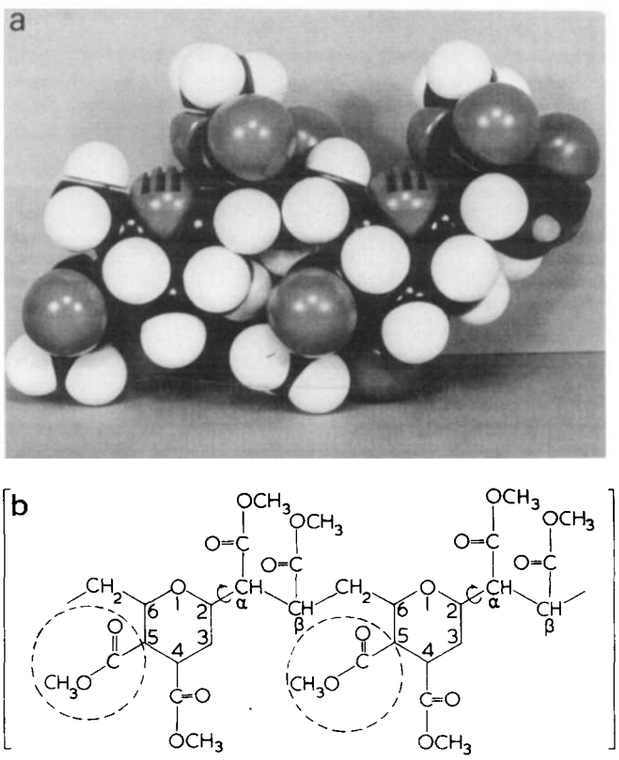

Figure 10 The molecular structure of DME(I): (a) Ealing CPK atomic model showing 2 monomer units: (b) schematic representation of 2 monomer units

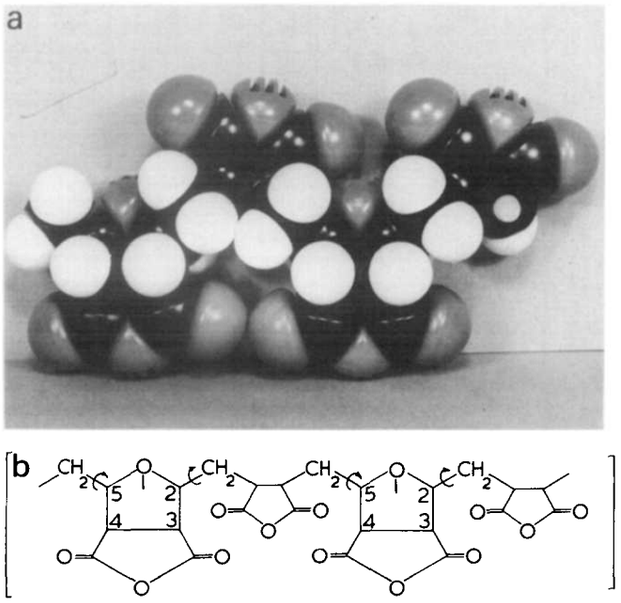

Figure 11 The molecular structure of DIVEMA(II): (a) Ealing CPK atomic model showing 2 monomer units: (b) schematic representation of 2 monomer units

ture (the two locations indicated by arrows in the above diagram and in *Figure 9*).

When esterification of DIVEMA(I) occurs, the anhydride rings open. This leads to a significant conformational change in the structure. The anhydride ring in the DIVEMA(I) structure has a compact conformation preventing steric interference to bond rotation. When, during esterification, the anhydride ring oxygen bond is opened, the anhydride carbons move apart to accommodate the bulky methyl ester groups. This results in steric interference to bond rotation. Rotation can still occur around the bond between the C-2 pyran carbon and the backbone α carbon [see DME(I) above and *Figure 10*]; however, rotation is blocked around the bond connecting the backbone chain CH_2 group adjacent to the C-6 pyran carbon. Not only is a larger volume occupied by the methyl ester groups than by the unreacted anhydride ring, but the angle of the C-5 pyran ring position tends to spatially direct the bulky ester group in the same direction as that of the CH_2-pyran C-6 bond. The result of this is that rotation around the CH_2-pyran C-6 bond is now blocked by interference between the ester group attached to the 5-position on the pyran ring and the ester group attached to the β main-chain carbon. This is indicated schematically by the broken line circle in the DME(I) diagram above (see also *Figure 10*). Thus the CPK model has shown that the accepted DME(I) structure has only one freely rotatable bond. A consequence of this is that the whole comonomer DME(I) must be considered as the 'virtual bond' in the characteristic ratio calculation, and as has already been shown this leads to an unreasonable numerical value for C_∞.

The conclusion that the accepted DIVEMA(I) structure was unsatisfactory led to a search for an alternate model for the DIVEMA molecule. Breslow[2] has pointed out that although the pyran ring structure for DIVEMA has been widely accepted, there is no convincing evidence for it. He suggests a DIVEMA structure containing the 5-membered tetrahydrofuran ring instead of the 6-membered tetrahydropyran ring as a possible alternative.

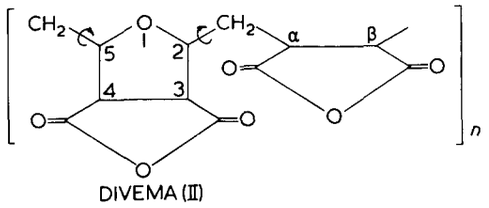

DIVEMA (II)

DIVEMA(II) was constructed using the CPK models. Formation of the tetrahydrofuran ring introduces another CH_2 group into the backbone chain, located between C-2 of the furan ring and the main chain anhydride ring α carbon (see above and *Figure 11*). This has two significant configurational consequences. First, it increases the distance between the main chain anhydride ring and the furan ring, and secondly, it changes the angular position of the main chain anhydride ring with respect to the furan ring. Also the furan ring in DIVEMA(II) directs its attached anhydride ring downward and not toward the adjacent main chain anhydride ring. The CPK model further shows (*Figure 11*) that the DIVEMA(II) structure, like the DIVEMA(I) structure, has two rotating main chain bonds, with rotation occurring around the backbone bonds connected to the 2- and 5-furan ring carbons [see DIVEMA(II) above and *Figure 11*].

Since the DIVEMA(I) and the DIVEMA(II) structures both have two rotating backbone bonds they would be expected to form similar random coils in solution. Thus DIVEMA'S solution properties would not be able to distinguish between the two models. Methyl esterification acts as a structural probe, however, which has already shown that the DME(I) structure is unlikely, since it yields an unreasonable characteristic ratio.

Methyl esterification of the DIVEMA(II) structure results in a significantly different steric structure from that of DME(I).

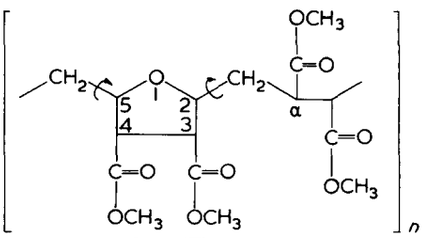

DME (III)

The CPK model of DME(II) has a more open structure than DME(I) [see *Figure 12*]. The increased room gained by the addition of a CH_2 group between the furan 2-carbon and the α backbone ester carbon, combined with the changed angular orientation of both the backbone esters with respect to the furan ring, and the ester attached to C-4 of the furan ring with respect to the β backbone ester group, leads to easy rotation around the bonds adjacent to both the C-2 and C-5 of the furan ring (see DME(II) schematic above and *Figure 12*).

With a knowledge of the bond rotation positions of the DME(II) molecule it is possible to calculate its characteristic ratio. The 'virtual' bonds of this copolymer now consist of two subunits; (A) around the furan ring and (B) over the rest of the chain.

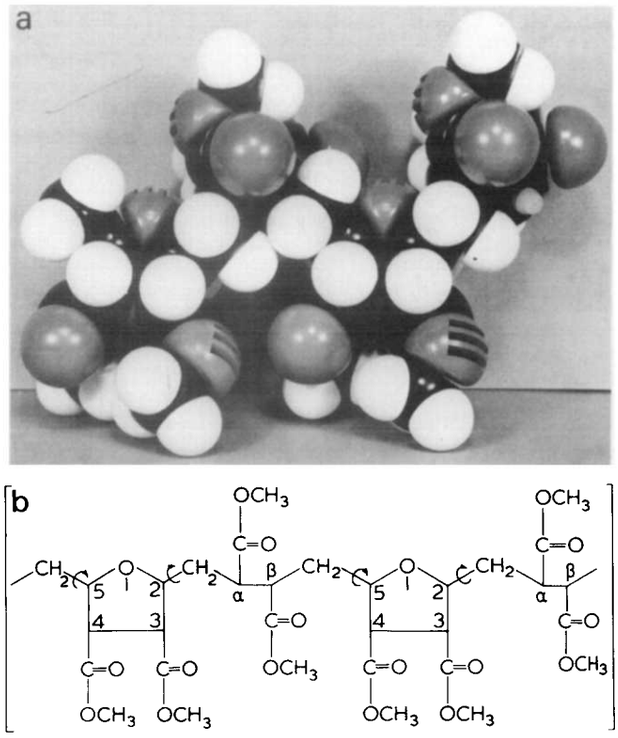

Figure 12 The molecular structure of DME(II): (a) Ealing CPK atomic model of 2 monomer units; (b) schematic representation of 2 monomer units

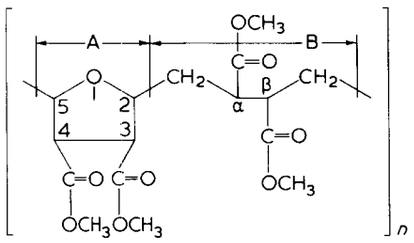

The flexible bond distance of this molecule is now the average distance between rotatable bonds, given by the average of the calculated values for A and B:

$$\left(\frac{M_b}{l^2}\right)_{\text{DME(II)}} = \left[\left(\frac{M_A}{l_A^2}\right) + \left(\frac{M_B}{l_B^2}\right)\right] \Big/ 2$$

$$= 13.37 \times 10^{16} \qquad (17)$$

where M_A is 186, l_A is 3.20×10^{-8} cm, M_B is 172, and l_B is 4.48×10^{-8} cm. Using this value of $(M_b/l^2)_{\text{DME(II)}}$ leads to a calculated value for the characteristic ratio of 4.59, i.e.:

$$C_\infty = \left(\frac{\langle r^2 \rangle}{M}\right)_\infty \left(\frac{M_b}{l^2}\right)_{\text{DME(II)}}$$

$$= (13.37 \times 10^{16})\,(0.3436 \times 10^{-16}) = 4.59 \qquad (18)$$

A characteristic ratio of 4.59 is certainly acceptable. It suggests the DME(II) chain is fairly flexible, a conclusion supported by the mobility of the CPK model of DME(II). It also shows that the DME(II) structure is experimentally satisfactory and is therefore the preferred model structure of the methyl ester.

It is unlikely that the internal ring structure of DIVEMA is modified by esterification. Thus the anhydride and the methyl ester should both have the same tetrahydrofuran ring structure. Although the experimental results do not eliminate the possibility of both tetrahydrofuran and tetrahydropyran rings coexisting in the DIVEMA structure, the low value of the characteristic ratio for DME, assuming only tetrahydrofuran rings present in the structure, suggests the tetrahydrofuran ring is the predominant structure in the DIVEMA chain. This conclusion is further supported by the CPK model observation that the DME(I) structure is a far more unwieldy, much less likely structure than DME(II), and therefore that the DME(II) structure is the energetically favoured structure.

CONCLUSIONS

This study serves as an excellent example of how substitution of bulky substituent groups can be used as a molecular probe to differentiate between different possible structural conformations. By esterifying DIVEMA it has been possible to produce a situation wherein the solution behaviour of the DME from one possible DIVEMA conformation would be very different from the other. This has led to the observation that DIVEMA most likely contains a tetrahydrofuran ring in the structure.

The study has also demonstrated the utility of the Universal GPC Curve in developing a g.p.c. calibration system for a new polymer whose available molecular weight range is limited. By demonstrating that narrow molecular weight fractions of divinyl ether–maleic anhydride methyl ester (DME) fit the Universal Curve for polystyrene standards it became possible to utilize the polystyrene standards for the DME evaluation. Also several new Mark–Houwink relations were obtained in the process of obtaining the necessary interaction parameters for utilizing the Universal curve. These included one for polystyrene in THF at 30°C:

$$[\eta]_{\text{PS}} = 1.328 \times 10^{-4}\, \bar{M}_w^{0.713}$$

and another for DME in THF at 30°C:

$$[\eta]_{\text{DME}} = 4.895 \times 10^{-4}\, \bar{M}_w^{0.50}$$

It is interesting to note that THF is a theta solvent for DME at 30°C; also, both the light scattering excluded volume data and the intrinsic viscosity–molecular weight results suggest some long chain branching may exist in the highest molecular weight fractions of DME. The fact that the DME data fit the g.p.c. universal calibration curve shows DME has a random coil configuration in solution.

ACKNOWLEDGEMENTS

The author acknowledges the assistance of R. H. Kridler who obtained the g.p.c., and viscosity data, L. G. Bunville for the light scattering results, O. W. Marks for the computer analysis of GPC, and D. S. Breslow and E. I. Edwards for samples and helpful discussions.

REFERENCES

1 Breslow, D. S., Edwards, E. I. and Newburg, N. R. *Nature* 1973, **246**, 160
2 Breslow, D. S. *Pure Appl. Chem.* 1976, **46**, 103
3 Keahey, S. J. personal communication
4 Butler, G. B. and Wu, C. *Polym. Sci. Technol.* 1973, **2**, 369
5 Benoit, H. C., Grubisic, Z., Rempp, P., Decker, D. and Zilliox, J. G. *J. Chim. Phys.* 1966, **63**, 1507
6 Butler, G. B., Corfield, G. C. and Aso, C. *Prog. Polym. Sci.* 1975, **4**, 129
7 Butler, G. C. *J. Polym. Sci. Polym. Symp.* 1975, **50**, 163
8 Marks, O. personal communication
9 Zimm, B. H. and Kilb, R. W. *J. Polym. Sci.* 1959, **37**, 19
10 Flory, P. J. 'Principles of Polymer Chemistry', Cornell University Press, New York, 1953, pp.531
11 Boni, K. A., Sliemers, F. A. and Stickney, P. B. *J. Polym. Sci. (A-2)* 1968, **6**, 1567, 1579
12 Coleman, M. M. and Fuller, R. E. *J. Macromol. Sci. (B)* 1975, **11**, 419
13 Ambler, M. R. and McIntyre, D. *J. Polym. Sci. (Polym Lett.)* 1975, **13**, 589
14 Flory, P. J. 'Statistical Mechanics of Chain Molecules', Interscience, New York, 1969, pp.37